Applicability of Hilbert-Huang Transform in Analysis of AC Grids Containing Power Electronic Devices

Anusha Srihari Arva, Bogdan Marinescu, Florent Xavier

Applicability of Hilbert-Huang Transform in Analysis of AC Grids Containing Power Electronic Devices

Anusha Srihari Arva
Centrale Nantes-LS2N-CNRS
Nantes, France
Email: anusha.arva@ls2n.fr

Bogdan Marinescu
Centrale Nantes-LS2N-CNRS
Nantes, France
Email: bogdan.marinescu@ls2n.fr

Florent Xavier
Réseau de Transport d'Électricité
Versailles, France
Email: florent.xavier@rte-france.com

***Abstract*—This paper studies the application of Hilbert Huang Transform (HHT) to oscillations generated by common power system phenomena. Firstly, an investigation was performed on the kind of damped modes that can be analyzed through HHT. HHT was then applied on signals from a nonlinear model of AC grid containing two close HVDC lines and power electronic devices. Two cases were studied: identification of coupling mode and temporal tracking of coupling mode during switching events. Results were compared with those obtained in modal analysis. In both cases it was found that HHT was able to provide better depth and clarity in off-line stability analysis.**

***Index Terms*—coupling modes, empirical mode decomposition, Hilbert Huang transform, instantaneous attributes, stability studies.**

I. Introduction

Vastly interconnected power systems of recent decades are often prone to oscillations of time varying frequency and amplitude, known as *nonstationary* oscillations. A common scenario where such oscillatory modes arise is when power converters are inserted into AC grids as in [1], giving rise to coupling modes. Damping of these modes depends heavily on power-flow and hence varies during operation. These modes are similar to the well-known inter-area modes in the sense that they are coupling modes (via the AC grid) between distant devices (power converters) but at higher frequencies (around 20Hz).

Application of conventional stability analysis techniques to nonstationary oscillations is found to have drawbacks such as loss of significant information due to linearization (modal analysis), assumption of stationarity (signal processing techniques such as Fast Fourier Transform (FFT)) and computational burden (curve fitting techniques such as Prony Analysis) [2],[4]. As an alternative, Hilbert-Huang Transform (HHT) which is an empirical data analysis technique designed specifically for analysis of nonstationary time series [3], can be used. HHT decomposes nonstationary nonlinear signals into their stationary components through Empirical Mode Decomposition (EMD) and defines *instantaneous* attributes through Hilbert Spectral Analysis (HSA) from which physically meaningful information about the signal can be extracted.

Extraction of modes using EMD and associated limitation have been investigated for a two-component test signal in [4]. The use of these results is not straightforward for analysis of power system oscillations because the test signal considered is undamped. In this case, the link with observability should be investigated. Major contribution of this paper is the extension of the aforementioned analysis by taking into account, the observability of the mode in conjunction with its frequency and damping. Results of this step are used as reference in subsequent steps of applying HHT to signals from a simulated non-linear model of AC grid containing power electronic devices. MATLAB® toolbox for HHT [5] and Simulink are used to perform necessary computations.

The paper is organized in the following way. Section II recalls the fundamentals of HHT. Section III elaborates on the investigation performed on HHT in case of damped oscillations. Section IV describes the empirical analysis performed to determine working ranges of HHT. Section V presents the application of HHT on AC grid containing coupling modes. Finally, Section VI concludes with key findings and future work.

II. Fundamentals of Hilbert-Huang Transform

Proposed by Huang *et al* in [3], HHT consists of two phases which are recalled in this section.

A. Empirical Mode Decomposition

Nonstationary signals consist of multiple modes of oscillation which need to be separated into their stationary equivalents. EMD decomposes the input signal into its constituent modes, namely, Intrinsic Mode Functions (IMF) through a process called *sifting* [3]. A signal is considered as an IMF if it satisfies the following conditions:

C1. The difference between the number of extrema (maxima and minima) and the number of zero crossings along the length of the signal is at most one.

C2. The mean value of the envelopes formed by local maxima and by local minima, at each point on the signal, is zero.

Given a real-valued input signal $y(t)$, following are the steps performed to obtain IMFs [4]:

S1. Identify local maxima and minima along the length of the signal.
S2. Connect local maxima and minima separately using cubic spline interpolation to construct upper $u(t)$ and lower $l(t)$ envelopes respectively.
S3. At each instant, compute the local mean of the upper and lower envelopes as: $m(t) = \left(\frac{u(t)+l(t)}{2}\right)$.
S4. Compute proto-IMF as $h(t) = y(t) - m(t)$.
S5. Check if $h(t)$ satisfies conditions C1 and C2. If not, repeat steps S1 to S5 by replacing $y(t)$ with $h(t)$ until the conditions are satisfied.
S6. If C1 and C2 are satisfied, set proto-IMF $h(t)$ as valid IMF $x(t)$.
S7. Compute residue $r(t) = y(t) - x(t)$ and repeat steps S1 to S7 until a trend is obtained.

The above steps result in IMFs in decreasing order of frequency which can be summed back to the input signal as:

$$y(t) = \sum_{i=1}^{n} x_i(t) + r_n(t). \tag{1}$$

B. Hilbert Spectral Analysis

Application of Hilbert Transform on each IMF requires real valued IMFs to be expressed as analytical signals as follows:

$$z(t) = x(t) + jx_H(t) = A(t)e^{j\theta(t)}. \tag{2}$$

where $j = \sqrt{-1}$, $z(t)$: analytical signal corresponding to $x(t)$, $x(t)$: real valued IMF and $x_H(t)$: Hilbert Transform of $x(t)$ computed according to the following definition:

$$x_H(t) = \frac{1}{\pi} P \int_{-\infty}^{\infty} \frac{x(\tau)}{t-\tau} d\tau. \tag{3}$$

where P: Cauchy's Principle value of the integral employed to avoid singularities.

Instantaneous Amplitude $A(t)$ (referred to as IA for clarity, in this paper) and *Instantaneous Phase* $\theta(t)$ are defined on the analytical signal in (2) as follows:

$$A(t) = \sqrt{(x^2(t) + x_H^2(t))} \quad \theta(t) = \tan^{-1}\left(\frac{x_H(t)}{x(t)}\right). \tag{4}$$

Instantaneous angular frequency $\omega(t)$ (referred to as IF, in this paper) is then defined as follows:

$$\omega(t) = arctan(z_i \overline{z}_{i+1}). \tag{5}$$

where $\overline{z}_{i+1}$: conjugate of analytical signal at time t_{i+1}, z_i: analytical signal at time t_i. This definition is implemented to avoid phase unwrapping required in the classical definition which is differentiation of $\theta(t)$ [8]. To obtain the frequency value in Hz, $\omega(t)$ is multiplied by $F_s/2\pi$ where F_s is the sampling frequency.

Regarding damped oscillations of power systems, decay rate of each IMF can be defined as [6]:

$$\sigma(t) = \frac{ln\left(\frac{A_{i+1}}{A_i}\right)}{\Delta t}. \tag{6}$$

where A_{i+1} and A_i are instantaneous amplitudes of each IMF computed by (4) at time instants t_{i+1} and t_i respectively. Using $\sigma(t)$ and $\omega(t)$, *instantaneous damping ratio* $\zeta(t)$ (referred to as ID, in this paper) can be computed using the standard definition (see, for example, [6]).

C. Numerical estimates of instantaneous attributes

In order to compute global quantities (frequency in Hz and the damping ratio) from instantaneous attributes, envelope mean is first computed on the IF and ID curves, followed by averaging of the upper and lower envelopes at each instant. Global mean is then computed along the length of the attribute to obtain a global estimate. This is done because direct computation of mean results in inaccurate values since Hilbert based computation is sensitive to minute variations in signals [7]. However, with envelope mean approach, better estimates can be obtained from sensitive instantaneous attributes.

D. Tools used to validate results of HHT

Two major validations that need to be done are:

- *Frequency of IMFs in Hertz*
  EMD decomposes nonstationary data into IMFs which are supposed to be monocomponent and in decreasing order of frequency. Each IMF is validated in frequency domain using FFT which is computationally inexpensive and most widely used frequency domain tool.
- *Number of useful components from decomposed IMFs*
  EMD performs simultaneous amplitude and frequency modulation of the input signal, making the last few IMFs overly modulated versions of the last valid component. Valid IMFs are determined using cross correlation, which is a measure of similarity between two signals, quantified by correlation coefficient which varies from 1 (the signals are exactly the same) to -1 (the signals are opposite in sign to each other). In this work, correlation coefficients are computed between each IMF and the input signal. The IMF is considered valid if the correlation coefficient is greater than a predetermined threshold of 0.5.

III. Investigation on HHT in case of damped oscillations

HHT is known to perform well in analysis of undamped input signals with necessary enhancements to the algorithm [4]. However, operation of nonlinear power systems needs also to track a number of damped oscillatory modes. As primary contribution, following challenges associated with damped modes were identified using a bimodal test system:

(a) Factors affecting the choice of the length of the signal chosen for analysis
(b) Quantification of modal parameters from instantaneous attributes
(c) Identification of relevant IMFs from the decomposed set of IMFs
(d) Link between detection of modes in EMD and their observability in a group of modes

Challenges (b) and (c) have been highlighted in [2] for a general case. However, this investigation encompasses overall challenges with focus on damped modes found in power

systems. To create damped modes, two second order transfer are used which are of the form:

$$Y(s) = Y_1(s) + Y_2(s),$$
$$Y_1(s) = \frac{\omega_1^2}{s^2+2\zeta_1\omega_1 s+\omega_1^2},\ Y_2(s) = \frac{\omega_2^2}{s^2+2\zeta_2\omega_2 s+\omega_2^2}. \quad (7)$$

where angular frequencies ω_1, ω_2 and damping ratios ζ_1, ζ_2 are varied to generate various damped modes. The input to HHT is the sum of step responses of $Y_1(s)$ and $Y_2(s)$ given by:

$$y(t) = y_1(t) + y_2(t). \quad (8)$$

HHT is applied on the sum of step responses of ($f_1 = 50$ Hz, $\zeta_1 = 5\%$) and ($f_2 = 10$ Hz, $\zeta_2 = 15\%$), with signal length of 0.3 s and sampling rate of 1 kHz (referred to as base case). For 0.3 s, FFT performed on the input signal gives two peaks at 49.83 Hz and 9.967 Hz, shown in Fig. 1. Instantaneous attributes and FFT of IMF1 and IMF2 are shown in Fig. 2 and Fig. 3 respectively. Instantaneous values of IA, IF and ID capture the temporal evolution of the amplitude, frequency and damping of the modes respectively.

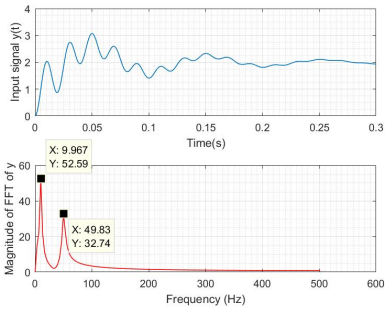

Fig. 1: Input signal and its FFT

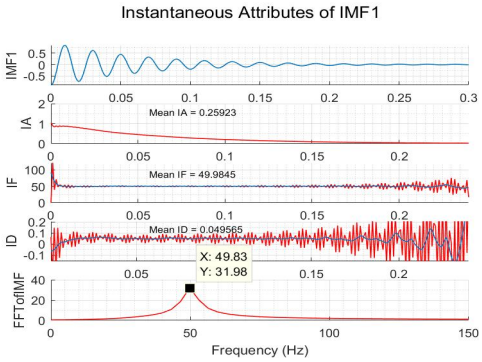

Fig. 2: Instantaneous attributes of IMF1

A. Choice of length of the signal for HHT

Two factors were found to affect the choice of length of the signal: settling times of relevant modes and computation of modal parameters (see Section III-B). A duration of 0.3 s is chosen in the base case so that the 10 Hz mode completes enough time periods for accurate determination of frequency. For modes of lower frequencies, longer lengths of signals are

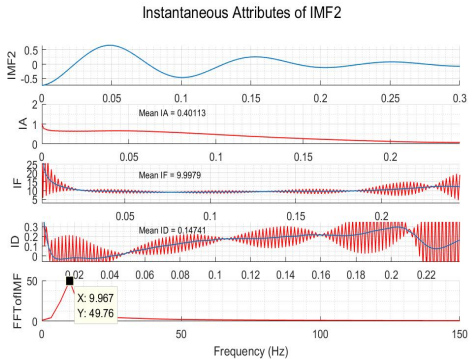

Fig. 3: Instantaneous attributes of IMF2

required and vice versa. In addition, there exists a trade off between the length of the signal for EMD and for FFT. This is seen in the deviation in numerical values of frequencies in Fig. 1 due to the sensitivity of FFT to length of the input signal. The longer the signal, better is the frequency estimate in FFT. On the contrary, EMD requires precise length of the signal (comparable to the settling time of the mode) for accurate decomposition. The question of choosing an appropriate length of the signal while accounting for the two factors is a challenging aspect that cannot be generalized at this stage of development. This calls for empirical choice of length of signal, making it difficult for application to unknown damped signals at this stage. However, HHT can be used effectively for applications involving off-line analysis of aforementioned type of signals.

B. Quantification of modal parameters from instantaneous attributes

Instantaneous attributes are considered until 0.24 s instead of 0.3 s for two reasons. First, end effects are known to occur in Hilbert based computation [3]. This can be eliminated successfully [9], [6] and is part of future work. Second, instantaneous attributes result in spurious values when there are no significant variations in the signal, that is, after the settling time of the damped mode, an observation which is also made in [2]. Mean value of IF computed for stable portions of curves (0.05 to 0.23 s) give 49.9845 Hz ($\approx$ 50 Hz) and 9.9979 Hz ($\approx$ 10 Hz) respectively. Numerical estimates for damping are computed for different windows considering the global variation of the signal. For IMF1, ID averaged from 0.02 to 0.18 s amounts to 0.049565 (4.9565% $\approx$ 5%). For IMF2, ID averaged from 0 s to 0.24 s was found to be 0.14741 (14.741% $\approx$ 15%). Although the computation indicates satisfactory accuracy, the same can be ensured only by fine tuning the lengths for each individual case, making it challenging to apply on unknown signals.

C. Identification of relevant IMFs

Identification of relevant IMFs in case of damped modes was resolved using correlation coefficients. Applying HHT on the input signal results in four IMFs whose correlation

coefficients in Table I indicate that IMF1 and IMF2 are valid relevant IMFs (coefficients greater than threshold value of 0.5).

TABLE I: CORRELATION COEFFICIENTS OF IMFs FOR BASE CASE

	IMF1	IMF2	IMF3	IMF4
Correlation coefficients	0.608	0.7725	0.3097	0.1323

However, in a group of modes with drastically different damping ratios, similarity of highly damped IMFs with the input signal may not be established, making this approach less reliable. This fact also motivates the study of the link between observability of damped modes and their detection in EMD.

D. Link between observability of modes and detection in EMD

By converting (7) into standard state space form (A,B,C,D), *Observability Index* (OI) of a given mode λ, in our example, is defined as:

$$OI = |C * v|. \tag{9}$$

where v is the right eigenvector associated to the mode λ of state matrix A. Observability indices are computed for each mode in the system to check dominance of a particular mode over the other in the response y. For comparison, *Relative Observability Index* (ROI) is defined as:

$$ROI = \frac{OI_1}{OI_2}. \tag{10}$$

where OI_1 and OI_2 are the observability indices of 50 Hz mode and 10 Hz mode respectively. Several combinations of modes were simulated and EMD was performed on the signal to examine the decomposition as well as link to observability of the mode. The most crucial cases are captured in Table II.

TABLE II: HHT ON MODES WITH DIFFERENT ROI

Case	Mode (f Hz, ζ %)	ROI	Detection in EMD
1	$f_1 = 50$, $\zeta_1 = 5$, $f_2 = 10$, $\zeta_2 = 15$	$\frac{9.2805}{3.7536} = 2.4724$	Both modes
2	$f_1 = 50$, $\zeta_1 = 80$, $f_2 = 10$, $\zeta_2 = 15$	$\frac{9.2805}{3.7536} = 2.4724$	Only 10 Hz mode
3	$f_1 = 50$, $\zeta_1 = 5$, $f_2 = 10$, $\zeta_2 = 80$	$\frac{0.0108}{0.0659} = 0.1642$	Only 50 Hz mode

It can be seen that modes detected in EMD in each case were those with low damping, despite their observability index being lower than the other mode. It can be concluded that detection in EMD is independent of observability of the mode in a group of modes. It depends solely on its damping and frequency combination which essentially determines the geometry of the input signal. This result therefore drives the empirical study of EMD in different ranges of frequencies and damping of modes.

IV. EMPIRICAL DETERMINATION OF FREQUENCY AND DAMPING RANGES OF MODES FOR EMD

In this work, extraction of modes through EMD was studied in three frequency ranges; Modes which are one octave apart are chosen in: low ($f_1 = 1$ Hz, $f_2 = 0.3$ Hz), mid ($f_1 = 50$ Hz, $f_2 = 10$ Hz) and high frequency ranges ($f_1 = 80$ Hz, $f_2 = 10$ Hz). Depending on settling times of the modes, length of the input signal in each case was: 10 s for low, 0.2 s for mid and high frequency ranges. Damping of each mode was varied while keeping the damping of the other mode constant at 5% and HHT was applied on the composite signal.

TABLE III: EMPIRICAL RANGES OF FREQUENCY AND DAMPING FOR CLEAR EMD

	f_1		f_2	
f \ ζ	$\zeta_{1_{min}}(\%)$	$\zeta_{1_{max}}(\%)$	$\zeta_{2_{min}}(\%)$	$\zeta_{2_{max}}(\%)$
Low	1.1	7	2.6	28
Mid	2.6	6.4	2.6	11.5
High	4.1	5	4.19	9.36

Table III captures the damping limits within which clear decomposition is possible in EMD. Decomposition was considered to be clear if following conditions were satisfied:

- Both frequencies f_1 and f_2 are detected distinctly in subsequent IMFs in the decomposition; indicated by FFT peak of highest magnitude
- IMFs are monocomponent in nature; indicated by a single peak in FFT of the IMF

For damping values outside these limits, EMD resulted in mode mixing, that is, small amplitude of the other IMF remains mixed in either or both IMFs (even though the two modes are an octave apart). Tracking the ROI of the modes across these ranges showed no visible pattern, proving once again that EMD is independent of observability of modes. EMD was found to work well over wider limits of damping in low frequency range while the limits become increasingly smaller when one moves to higher ranges. These results substantiate the increased use of HHT in analysis of low frequency, particularly inter-area oscillations.

The working range of EMD determined in this analysis provides a valuable perspective on the kind of damped modes in non-linear time varying systems that can be analyzed through HHT. The working range can be used to choose modes of practical importance, particularly lowly damped modes, for off-line analysis.

V. APPLICATION OF HHT TO AC GRID MODEL CONTAINING POWER ELECTRONIC DEVICES

This section presents the application of HHT in two cases: identification of coupling mode in the linearized system and temporal tracking of coupling mode during switching event.

A. System description

AC grid considered for analysis in this paper consists of two two-level HVDCs interconnected through a common AC power line [1]. Each HVDC link has two conversion stations that employ bidirectional 3-phased AC-DC power converters, as seen in Fig. 4. Insertion of power converters into the AC grid gives rise to coupling mode whose damping may vary depending on the level of active power injected by AC-linked stations into the grid. Coupling mode of around 20 Hz was identified in the modal analysis of the system linearized around various operating points [1]. This is used as the basis for comparison with HHT analysis (Tables IV and V).

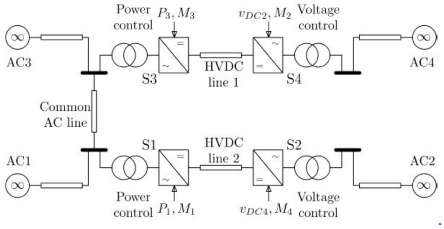

Fig. 4: AC grid containing two close HVDC links and power electronic devices

B. Identification of Coupling Mode in the linearized model

Operating condition chosen is such that 600MW of power is injected into the AC line by setting the reference values of VSCs at stations S1 and S3. Modal Analysis on the linearized model resulted in 16 modes ranging from 87.34 Hz (with $\zeta = 8.6\%$) to 4.35 Hz (with $\zeta = 91.3\%$), some of which are shown in Table IV. Based on the working range of EMD in Table III, the modes are classified with respect to their detection in HHT. Out of the full set of modes active around the operating point, the 19.54 Hz mode is expected to be seen in HHT. Two other modes are probable to be detected due to their damping being close to the limit in the low frequency range. With this estimation made, HHT was applied on the step response of the linearized system, shown in Fig. 5(a).

TABLE IV: ESTIMATION OF DETECTION OF MODES BASED ON EMPIRICAL RANGES

f (Hz)	ζ (%)	Detection	Reason
87.34	8.6%	No	Very high f, ζ out of limit
19.54	**1.7%**	**Yes**	**Mid range f, ζ within limit**
18.93	66.9%	No	Mid range f, ζ out of limit
5.69	32.1%	Probable	Low f, ζ close to limit
5.65	30.7%	Probable	Low f, ζ close to limit
4.35	91.3%	No	Low f, ζ out of limit

FFT revealed two components: the coupling mode of 19.54 Hz and 0.4341 Hz which can be attributed to the trend signal upon which 19.54 Hz mode is superimposed. Three IMFs were obtained in EMD with correlation coefficients: 0.509, 0.2461 and 0.6252 respectively. IMF1 contains the relevant information where as IMF3 refers to the trend. Fig. 5(b) shows the first IMF containing the coupling mode. Temporal evolution of all instantaneous attributes are captured, where their actual values are plotted in red and their envelope means are plotted in blue. Mean is computed on IF and ID from 0.1 s to 1.5 s taking into account the settling time of the mode and excluding the end effects. Mean IF and mean ID were found to be 19.5431 Hz and 0.017568 (1.7568%) respectively which match the results of modal analysis up to two decimal places. It is evident that HHT is not only able to identify coupling modes in nonlinear AC grids but also provide their temporal evolution, giving it an edge over conventional modal analysis.

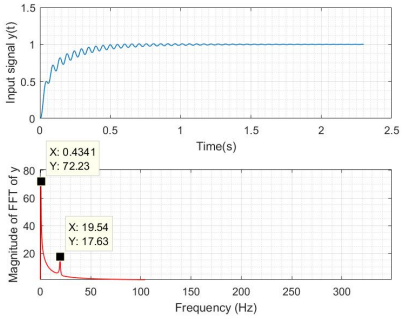

(a) Input signal and its FFT

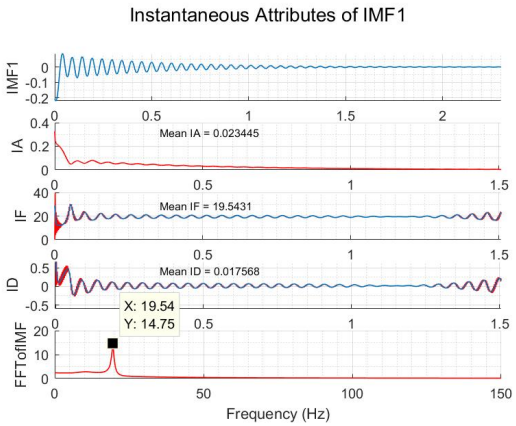

(b) IMF1 which contains the relavent mode

Fig. 5: HHT applied to identify and track coupling mode

C. Temporal tracking of coupling mode in case of switching events

A switching event was simulated by changing the reference level of the VSCs at S1 and S3 to inject 300MW of power into the grid at 8 s and another step increase from 300 MW to 600 MW was done at 8.4 s. The voltage signal ($M3 = V_3 + \lambda Q_3$) was chosen as the input to HHT with the objective of checking the extent of information that can be provided by HHT when applied on any non-linear signal sampled from a system undergoing a switching event. Following the modal analysis and estimation procedure similar to Subsection V-B, coupling mode identified in the system after the second switch was found to be 19.64 Hz as shown in Table V. The signal M3 from 8 s to 10.8 s was chosen to be analyzed through HHT as shown in Fig. 6.

TABLE V: COUPLING MODE IDENTIFIED IN MODAL ANALYSIS AFTER THE SECOND SWITCHING EVENT

f (Hz)	ζ (%)	Detection	Reason
19.64	2.6%	Yes	Mid range f, ζ within limit

Correlation coefficients of the IMFs in Table VI indicate that IMF1 is the only relevant IMF. Fig. 7 shows the evolution of the coupling mode when switching events were triggered. FFT of the input signal and of the IMF confirm that the dominant mode in the signal is 19.64 Hz which is the same as the

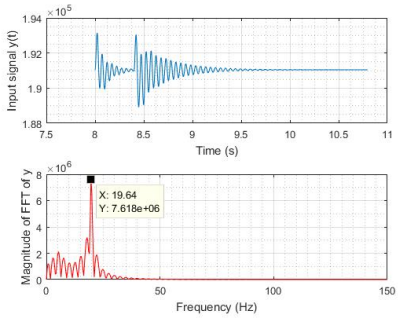

Fig. 6: Signal M3 in the switching event and its FFT

TABLE VI: CORRELATION COEFFICIENTS OF IMFs FOR POWER SIGNAL IN CASE OF SWITCHING EVENT

	IMF1	IMF2	IMF3	IMF4	IMF5	IMF6
Correlation coefficients	0.8571	0.01667	0.01626	0.04375	0.01703	0.04817

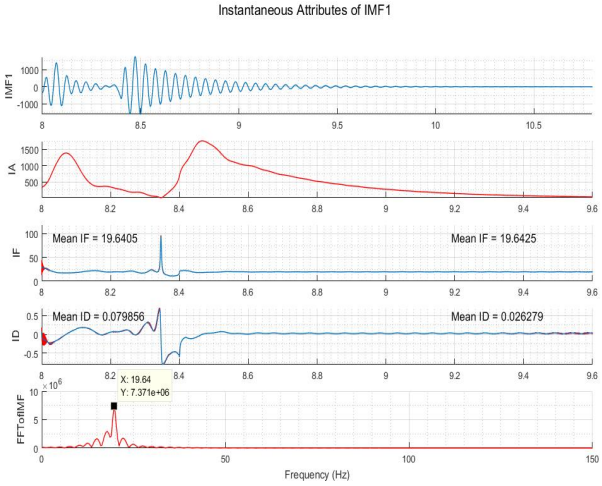

Fig. 7: Evolution of coupling mode in case of switching event

mode identified in modal analysis. Change in dynamics due to the second switching event is evident in all the instantaneous attributes between 8.3 and 8.5 s. IF and ID are averaged to obtain the numerical estimates before (8.0657 to 8.3 s) and after (8.7 to 9.6 s) the second switching event while considering the decay of the oscillations. Sharp change in IF indicates the trigger of new oscillations following those from the first event. Mean IF computed before and after the second switching event were found to be accurate up two decimal places. ID curve shows the evolution of damping of oscillations which is 7.9856% for the first switching event and 2.6279% for the second event (also verified by Modal analysis). Potential regions of instability are indicated by negative values of ID from 8.3 to 8.5 s indicating the instantaneous rise of perturbations before reaching a stable level at 8.5s. Low damping ratio of the oscillations from second switching event emphasizes the need for better control measures to reduce the threat to system stability.

VI. Conclusion

In this work, applicability of HHT in identification and tracking of damped modes typically found in power systems, was explored. The study of EMD on a composite signal containing damped modes proved that the likelihood of detection of a mode in HHT is independent of its observability. Hence, the range of modes that can be identified using HHT was determined empirically in terms of their damping and frequency combination. This investigation also reaffirmed the effectiveness of HHT in treating signals in the low frequency range.

Further, coupling modes in a nonlinear AC grid containing power electronic devices were analyzed through HHT. It was found that HHT was able to provide appreciable depth and precision in stability studies as compared to modal analysis. HHT was not only able to identify the crucial coupling modes but also track their oscillatory dynamics in case of switching events.

Challenges that are yet to be addressed are: development of algorithms to determine the length of the signal to be used in case of damped modes, implementation of solutions to problems already known in HHT such as end effect, mode mixing etc. Next stage involves using enhanced decomposition techniques such as masking based EMD in analysis of more complicated data which shall be presented in future work.

References

[1] I. Munteanu, B. Marinescu and F. Xavier, Analysis of the interactions between close HVDC links inserted in an AC grid, *IEEE PES General Meeting*, Chicago, IL USA, July 16-20 2017.

[2] T.J. Browne, V. Vittal, G.T. Heydt, A.R. Messina, Practical Application of Hilbert Transform Techniques in Identifying Inter-area Oscillations, *Inter-area Oscillations in Power Systems: A Nonlinear and Nonstationary Perspective*, ed. Arturo Roman Messina, ISBN 978-0-387-89529-1, pp. 63-100, 2009.

[3] N. E. Huang *et al*, The empirical mode decomposition and the Hilbert spectrum for nonlinear and nonstationary time series analysis, *Proc. Royal Soc.* London, 454:903995, 1998.

[4] D.S. Laila, A.R. Messina and B.C. Pal, Variants of Hilbert Huang Transform with Applications to Power Systems Oscillatory Dynamics, *Inter-area Oscillations in Power Systems: A Nonlinear and Nonstationary Perspective*, ed. Arturo Roman Messina, ISBN 978-0-387-89529-1, 2009.

[5] G. Rilling, *Empirical mode decomposition MATLAB codes with examples*, http://perso.ens-lyon.fr/patrick.flandrin/emd.html

[6] Y. Li *et al*, Oscillatory Parameters Computation Based on Improved HHT, *Interconnected Power Systems: Wide-Area Dynamic Monitoring and Control Applications*, Heidelberg, Germany, ISBN 978-3-662-48625-2, pp. 39-58, 2016.

[7] D.S. Laila, M. Larsson, B. C. Pal and P. Korba, Nonlinear damping computation and envelope detection using Hilbert Transform and its application to power systems wide area monitoring, *IEEE Power & Energy Society General Meeting*, Calgary, AB, Canada, 26-30 July 2009.

[8] M. Feldman, Analytic Signal Representation in *Hilbert Transform Applications in Mechanical Vibration*, 1st ed., John Wiley & Sons, ISBN: 978-0-470-97827-6, pp. 9-21, 2011.

[9] P. Li *et al*, Hilbert-Huang transform with Adaptive Waveform Matching Extension and its Application in Power Quality Disturbance Detection for Microgrid, *Journal of Modern Power Systems and Clean Energy*, Vol. 4, Issue 1, pp 19-27, 2016.